

Article ID: 1006-8775(2012) 03-0297-08

SIMULATION OF SPATIO-TEMPORAL DISTRIBUTION CHARACTERISTICS AND RADIATIVE FORCING OF ORGANIC CARBON AEROSOLS IN CHINA

SU Xing-tao (宿兴涛)¹, WANG Han-jie (王汉杰)², ZHOU Lin (周 林)¹

(1. Institute of Meteorology, PLA University of Science and Technology, Nanjing 211101 China; 2. Key Laboratory of Regional Climate-Environment Research for Temperate East Asia, Chinese Academy of Science, Beijing 100029 China)

Abstract: The International Centre for Theoretical Physics (ICTP, Italy) Regional Climate Model version 3.0 (RegCM3) is used to simulate spatio-temporal distribution characteristics and radiative forcing (RF) of organic carbon (OC) aerosols in and around China. The preliminary simulation results show that OC aerosols are mostly concentrated in the area to the south of Yellow River and east of Tibetan Plateau. There is a decreasing trend of column burden of OC aerosols from south to north in China. The maximum value of column burden of OC aerosols is above 3 mg/m² and located in the central and southern China, southeastern Tibet, and southwestern China's Yunnan, Guizhou, Sichuan provinces. The simulation on the seasonal variation shows that the maximum value of column burden of OC aerosols appears in winter and the secondary value is in spring and the minimum in summer. The RF of OC aerosols which varies seasonally is negative at the top of the atmosphere (TOA) and surface. The spatio-temporal characteristics of the RF of OC aerosols are basically consistent with that of IPCC, implying the high accuracy of the parameterization scheme for OC aerosols in RegCM3.

Key words: organic carbon aerosols; RegCM3 model; column burden; radiative forcing; numerical simulation

CLC number: P435

Document code: A

1 INTRODUCTION

There are three kinds of carbon aerosols in the atmosphere^[1]: organic carbon (OC), carbonate carbon (CC) and elemental carbon (EC). Black carbon (BC) and EC are physically the same matter though they are defined differently^[2]. Organic aerosols are complex mixture of chemical compounds containing carbon-carbon bonds produced from fossil fuel and biofuel burning and natural biogenic emissions. OC aerosols are emitted as primary aerosol particles which come from inadequate burning of fossil fuel and biofuel or formed as secondary aerosol particles from condensation of organic gases that are considered semi-volatile or having low volatility^[3]. OC is an atmospheric infectant which can be inbreathed into the human lung, so it can do great damage to environment and human health. The hygroscopicity of OC can also be changed by absorbing sulfate and nitrate aerosols, greatly contributing to the concentrations of atmospheric

cloud condensation nuclei (CCN). Therefore, OC plays an important role in global climate change by altering global radiation balance, and it has been one of the most uncertain factors in climate forecasting^[4].

Though OC aerosols are studied relatively late in China, many valuable conclusions have been achieved. Zhang et al.^[3] investigated the transport and transformation processes of OC aerosols over East Asia in the spring of 2001 with a regional three-dimensional chemical transport model. Simulation results showed that high levels of column burden of OC aerosols concentrate in the middle reach of Yangtze River and southwestern China, and the model reproduces the distribution characteristics of OC aerosols reasonably well as compared to observation data. Han et al.^[5] simulated the distribution characteristics of OC aerosols over China in July and August in 2003 with a regional air quality model system (RAQMS). The results indicated that high concentration of OC aerosols mainly occur in the

Received 2010-09-28; **Revised** 2012-05-09; **Accepted** 2012-07-15

Foundation item: National Fundamental Research Program of China (2011CB403202); National Natural Science Foundation of China (40675040)

Biography: SU Xing-tao, Ph.D. candidate, primarily undertaking research on aerosols and regional climate simulation.

Corresponding author: SU Xing-tao, e-mail: suxingtao@sina.com

areas along the Yangtze River, central southern China and most parts of north China, with the maximum of monthly mean concentration as high as $15 \mu\text{g}/\text{m}^3$. Cao et al.^[6] presented detailed high-resolution emission inventory of OC in China in the year 2000. The calculated emission was 4100 Gg for OC, mainly due to the burning of coal and biofuel. In addition, Lü et al.^[7] studied the effect of calcium sulfate and ammonium sulfate aerosols on secondary organic aerosol (SOA) formation. The results indicated that SOAs were generated in m-xylene/ NO_x /air mixtures upon ultraviolet light irradiation. The presence of CaSO_4 aerosols in the system was found to have no effect on SOA yields, whereas the presence of $(\text{NH}_4)_2\text{SO}_4$ aerosols can increase SOA yields. The outcome of this work can be applied to correct air quality model. Cao et al.^[6] pointed out the significance in OC aerosols studies and reviewed the main progresses. The research emphasizes that, in the future, special attention should be paid on spatio-temporal distribution of observation, emission inventory compilation, chemical character analysis, atmospheric chemical effects and the techniques used to reduce or control the emission of OC aerosols and so on.

China is considered to be the country that emits most OC aerosols in the world by some scholars^[8-10]. Moreover, due to the unique geographic position and fast development of social economy, the OC emission varies significantly annually, seasonally, monthly or even daily, and it is thus difficult to confirm the spatio-temporal distribution of OC aerosols exactly. Although the Chinese scientists paid special attention to OC aerosols associated with the climate change in recent years, the understanding of which is still limited. Few researches are restricted to the analysis method and spatio-temporal variation and pollution consequence in different cities (e.g., Chongqing^[11-12], Beijing^[13], Taiyuan^[14]) during different periods. Systemic and durative research is absent, especially on the radiative effects of OC aerosols in China. In this work, we use a regional climate model RegCM3 to simulate spatio-temporal distribution characteristics and radiative forcing of OC aerosols in and around China, which should be used as the reference for future study on the impacts of OC aerosols on the regional climate change in China.

2 METHODS AND DATA

2.1 Model description

RegCM3 is the third generation regional climate model developed by Abdus Salam International Centre for Theoretical Physics (ICTP), Italy, based on the RegCM and RegCM2. In RegCM3, CCM3 radiation scheme is used for radiation calculations^[15] with improvements in the role of atmospheric aerosols.

Referring to the method of Kiehl et al.^[16], all optical parameters including specific extinction, single scattering albedo and asymmetry parameter of different aerosols in 18 shortwave band ($0.2\sim 5.0 \mu\text{m}$) are defined. The aerosols optical depth (AOD) of OC is calculated by Eqs. (1) and (2).

$$\tau_l = 1.0 \times 10^5 \times m_r \times path \times e_l \times (1 - r_h)^{-0.2} \quad (1)$$

$$\tau_b = 1.0 \times 10^5 \times m_r \times path \times e_b \quad (2)$$

where τ_l is the AOD of hygroscopic OC, and τ_b the AOD of hydrophobic OC. In RegCM3 model, the ratio of hygroscopic to hydrophobic OC aerosols is 1:1 and the turnover time from hydrophobic OC to hygroscopic OC is 1.15 day. e_l is the specific extinction of hygroscopic OC aerosols, e_b the specific extinction of hydrophobic OC aerosols, r_h the relative humidity. $path = (p_{k+1} - p_k) / g$, p_{k+1} and p_k are respectively the interface pressure of $k+1$ level and k level in the model, m_r is the mass mixing ratio and is defined as:

$$m_r = \frac{g \times \tau_\lambda}{10^4 \times k^* \times rhfac \times (1 - \omega^* g^*) \times (p_s - p_{\max})} \quad (3)$$

where g is the gravitational acceleration, τ_λ the AOD in visible wave band ($0.5\sim 0.7 \mu\text{m}$ in RegCM3), k^* the specific extinction, ω^* the single scattering albedo, g^* the asymmetry parameter, $rhfac$ the regulating coefficient (1.6718), p_s the surface pressure, p_{\max} the pressure in the maximum height which aerosols can reach

The radiative forcing (RF) of OC aerosols at the surface and TOA can be deduced from the AOD of OC, which are calculated by:

$$RF_{TOA} = F_{TOA}(OC) - F_{TOA}(0) \quad (4)$$

$$RF_{SUR} = F_{SUR}(OC) - F_{SUR}(0) \quad (5)$$

where RF_{TOA} is the RF at the TOA, RF_{SUR} the RF at the surface, $F_{TOA}(OC)$ and $F_{SUR}(OC)$ the radiation fluxes at the TOA and surface respectively when OC aerosols are taken into consideration, $F_{TOA}(0)$ and $F_{SUR}(0)$ the radiation fluxes at the TOA and surface respectively when no OC aerosols are considered.

2.2 Aerosols data

The OC aerosol data (the resolution of emission inventory is $1^\circ \times 1^\circ$) is obtained from the official website of ICTP^[17]. The sources of OC aerosols are from human activity, fossil fuel burning and biomass burning. The monthly averaged emission inventory

comes from Liousse^[18].

2.3 Experiment design

The center of the model domain is set at 35°N, 114°E, with a grid space of 60 km, 76 grids in the north-south direction and 64 grids in east-west direction covering the entire East Asia continent (Figure 1). The model atmosphere is vertically divided into 18 layers, the model top is set at 50 hPa, the integration time-step is 200 s, and the buffer zone is set to 12 horizontal grids for each side of the domain. The Grell scheme is used for cumulus convection parameterization. The exponential relaxation and time dependent scheme is used for lateral boundary treatment. The initial and lateral boundary conditions are provided with NCAR/NCEP reanalysis data. The resolution of NCAR/NCEP data is 2.5°×2.5°, and the lateral boundary condition is updated at 6-h intervals. The vegetation/land use data is derived from the weekly averaged Global Land Cover Characterization (GLCC) dataset. The sea surface temperature data is obtained from the NCEP, updated weekly.

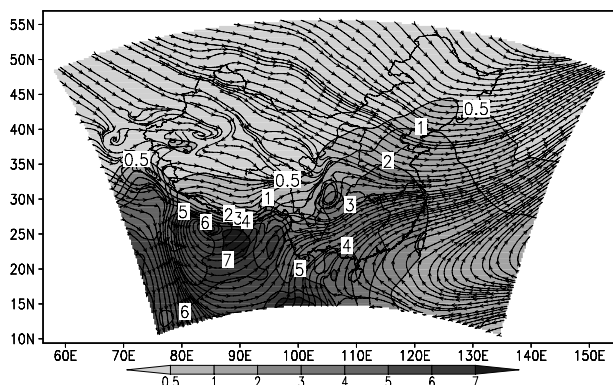


Figure 1. Column burden of OC aerosols (shaded area; units: mg/m^2) over the simulation domain and averaged horizontal transportation field between 850-700 hPa (stream line) in 2000.

The model run started at 0000 UTC December 1 in 1999 and ended at 0000 UTC January 1 in 2001. The model outputs of the first month run were omitted from the data analysis as the spin-up period, while the simulation results of the year 2000 were analyzed.

3 DISTRIBUTION CHARACTERISTICS OF OC AEROSOLS

3.1 Yearly averaged distribution

The simulated column burden distribution of OC aerosols in the year 2000 is shown in Figure 1. High values of OC aerosols in East Asia are mainly located at the Indochina Peninsula, the North Indian Plain, and the Bangladesh-India borders (the column burden is larger than $7 \text{ mg}/\text{m}^2$). The column burden of OC aerosols in and around China is smaller as compared with the above-mentioned regions. Rather larger

values occur in areas to the south of Yellow River and to the east of Tibetan Plateau. The maximum value of column burden of OC aerosols within China is about $3\text{--}5 \text{ mg}/\text{m}^2$, which is in the southern China's Yunnan, Guizhou and Sichuan province, and in the central southern China and southeastern Tibet. The column burden is between $2\text{--}3 \text{ mg}/\text{m}^2$ in the middle and lower reaches of Yangtze River and in the coast area of southeastern China. It is lower than $0.5 \text{ mg}/\text{m}^2$ in northern Tibetan Plateau, northwestern China, and in most of northeastern China and Inner Mongolia Autonomous Region.

Figure 2 shows the meridian (90–120°E) averaged distribution of OC aerosols in the year 2000. There is a decreasing trend from south to north. The mean value of column burden is $3.5 \text{ mg}/\text{m}^2$ at 20°N, but it reduces sharply to $0.5 \text{ mg}/\text{m}^2$ at 40°N.

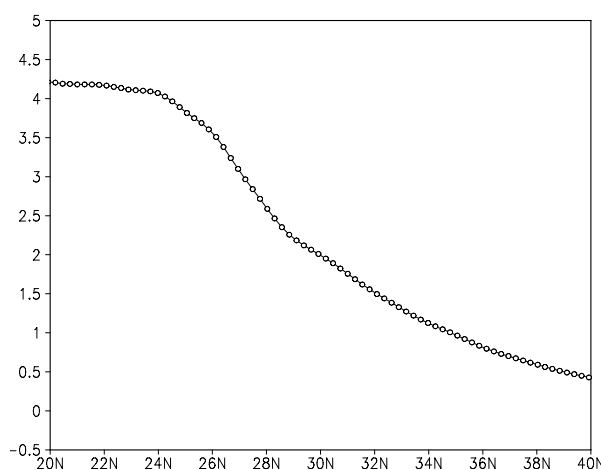


Figure 2. The meridian averaged distribution of column burden of Chinese OC aerosols in the year 2000 (units: mg/m^2).

The OC aerosol distribution characteristics can be explained based on the emission sources in China. Residential, industry and biomass burning are three main sources of OC aerosols in China (Table 1). Considering the population density and industry development, the eastern and southern China is more developed than the western and northwestern China, and the emission of OC aerosols from residential and industry are relatively large. Moreover, compared to the agricultural system “one or two crops a year” in northern China, the “two or three crops a year” system in southern China emits more OC aerosols. The complex topography, high mountains and hills, and weak wind resist the diffusion and transportation of OC aerosols, which attributes to considerably high column burden of OC aerosols in the Sichuan Basin.

Table 1. The estimated emissions (10^4t) and percentage of each emission source to total OC aerosols in 2000 (Cited from Cao et al.^[6]).

Emission sources	Power generation	Transportation	Biomass burning	Industry	Residential
Estimated emission	0.98	3.84	42.59	111.61	265.08
Percentage	0.2%	0.9%	10.0%	26.3%	62.6%

In addition, located in Asian monsoon region, dense emission sources and distinct atmospheric circulation in different seasons in East Asia result in crossing-border aerosol transportation to distant regions. Since OC aerosols are mostly concentrated in the low layers, the average transportation field of OC aerosols between 850–700 hPa needs to be investigated^[19]. As shown in Figure 1, the transportation direction is from southwest to northeast to the south of 30°N . Blocked off by Tibetan Plateau, OC aerosols from the north Indian Plain and the border between Bangladesh and India is driven into central southern China and middle and lower reaches of Yangtze River by southwest Asian monsoon. Meanwhile, OC aerosols from Indochina Peninsula are driven into the south of China by the southwest monsoon system as well. As two of the most populated areas around the world, India and Indochina Peninsula are emitting more and more OC aerosols with fast development of economy. These OC aerosols are mainly produced by residential, industry and biomass burning. Partly due to the transportation of OC aerosols from these regions, the concentration of OC aerosols in the south of China are considerably high. The Chinese government and scientific community should pay special attention to this reality in the diplomatic dialogue on climate change.

The southern Tibetan Plateau is also occupied by high concentration of OC aerosols. This phenomenon is attributed to the intense human activities of India. From the result of previous study, topography plays an important role in the distribution of aerosols. Driven by the high level circulation and blocked off by the Himalayas and Hengduan Mountains, the OC aerosols from India are accumulated in this region. This reflects the reality of transnational aerosol transportation.

3.2 Seasonal averaged distribution

Figure 3 presents seasonal distribution of column burden of OC aerosols in China of 2000. During spring, high column burden occurs in southern Guangdong and Guangxi with the maximum value above 5 mg/m^2 , with the column burden descending from south to north. The secondary maximum is located in southern Yunnan province and southeastern Tibet with values larger than 4 mg/m^2 . In addition, the column burden is generally above 3 mg/m^2 to the

south of Yangtze River and between $2\text{--}3\text{ mg/m}^2$ in the reach of Huaihe River and Jianghuai Basin. During summer, the column burden is far lower than that in spring to the south of Yellow River and the east of Tibetan Plateau. The maximum occurs in southern Guangdong and Guangxi with a value above 2.5 mg/m^2 . The secondary maximum is in the Sichuan Basin, Guangdong, Guangxi, Hunan, Hubei, Henan and Anhui with values larger than 2 mg/m^2 . In fall, the maximum of more than 3 mg/m^2 occurs in southeastern Tibet, Guangxi and Sichuan and central southern China. In winter, there is a descending trend of column burden from southwest to northeast in the southern region of Yellow River. The maximum is in southern Yunnan with a value larger than 7 mg/m^2 , and it rapidly reduces to $1\text{--}2\text{ mg/m}^2$ in the middle and lower reaches of Yellow River and Jianghuai Basin. The isoline of 0.5 mg/m^2 is expanded to Mongolia in summer and retreated to the lower reach of Yellow River in winter, which is mainly due to the winter monsoon.

The distribution of high column burden of OC aerosols in spring and summer is consistent with previous reports by Zhang et al.^[3] and Han et al.^[5].

As shown in Table 2, the simulation results show significant seasonal variation characteristics, the maximum of 3.03 mg/m^2 appears in winter, the secondary maximum 2.87 mg/m^2 in spring and the minimum 1.48 mg/m^2 in summer.

Besides the emission sources, the activities of weather systems also lead to seasonal variation characteristics. During spring, weakening winter monsoon, enhancing subtropical high and steady synoptic condition help keep relatively high concentrations of OC aerosols. Abundant precipitation plays an important role in washing out OC aerosols in summer, and strong monsoon from the ocean drives much clearer air into the mainland of China, leading to the minimum value of column burden in summer. During autumn, biofuel combustion is the main source of OC aerosols. But in winter, residents use more coal for heating than other seasons, which results in the highest value of column burden of OC aerosols, particularly in northern China.

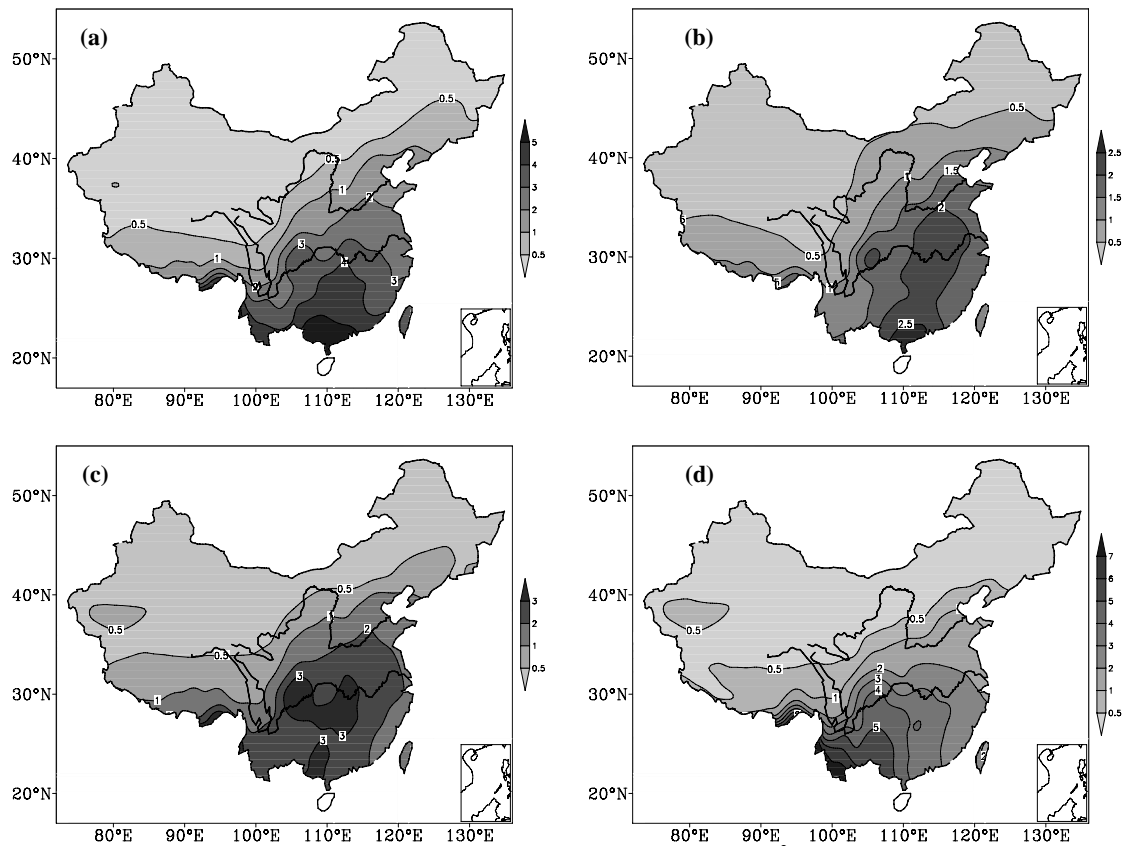


Figure 3. Seasonal distribution of column burden of OC aerosols in 2000 (units: mg/m^2). (a) spring; (b) summer; (c) autumn; (d) winter.

Table 2. Regional averaged column burden of OC aerosols for different seasons (units: mg/m^2).

Season	Spring	Summer	Autumn	Winter
Column burden	2.87	1.48	2.03	3.03

4 RADIATIVE FORCING OF OC AEROSOLS

4.1 Radiative forcing at the top of the atmosphere

Because of uncertainties in the estimation of radiative properties of aerosols, the study of RF of OC aerosols is far from adequacy. On the global scale, the RF of OC aerosols is $-0.41 \text{ W}/\text{m}^2$ by IPCC^[4], while it is merely -0.04 to $-0.06 \text{ W}/\text{m}^2$ by Jacobson^[20]. This may be due to enhancing absorbency of OC aerosols when mixed with BC aerosols. Meanwhile, Jacobson^[20] stated that the decrease of OC and BC emissions can restrain global warming more effectively than CO_2 . Simulation results indicate that the RF of OC aerosols is -0.32 to $-0.46 \text{ W}/\text{m}^2$ in clear sky and -0.70 to $-0.96 \text{ W}/\text{m}^2$ in cloudy sky respectively in 2050 in East Asia^[21].

Due to many uncertainties in calculating RF of OC aerosols, the present RegCM3 model only takes into account the direct effects of aerosols. The annual and seasonal averaged distribution of RF at the TOA in the year 2000 is shown in Figure 4 and Figure 5 respectively. Compared with Figure 1 and Figures 3-5, the distribution of RF at the TOA is consistent with

that of column burden. The yearly averaged distribution shows that there is a descending trend of RF from south to north. The maximum is in Guangxi, Yunnan and southeastern Tibet with values smaller than $-0.5 \text{ W}/\text{m}^2$, whereas the RF is about -0.1 to $0 \text{ W}/\text{m}^2$ in great parts of China including Tibetan Plateau, Xinjiang Uigur Autonomous Region, Mongolia and northeastern China. Referring to the seasonal distributional pattern, the maximum is in southeastern and southern parts of China in spring and summer, and there is a descending trend from southeast to northwest. With the summer monsoon enhancing, OC aerosols are driven into northern China, and the maximum is expanded to the middle and lower reaches of Yellow River. Along with the increase of the intensity of winter monsoon, high values of RF are retreated to the southern China and southwestern China. The maximum is concentrated in Sichuan Basin, Hunan and Guizhou in autumn while in Yunnan and Guangxi in winter. Due to the influence of clouds, surface albedo etc., the complex relationship of RF to AOD of OC aerosols may lead to the occurrence of positive RF in some regions.

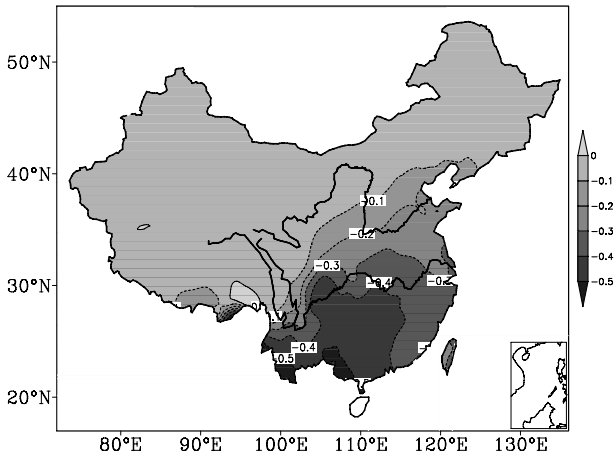


Figure 4. Yearly averaged distribution of RF at the TOA (units: W/m^2).

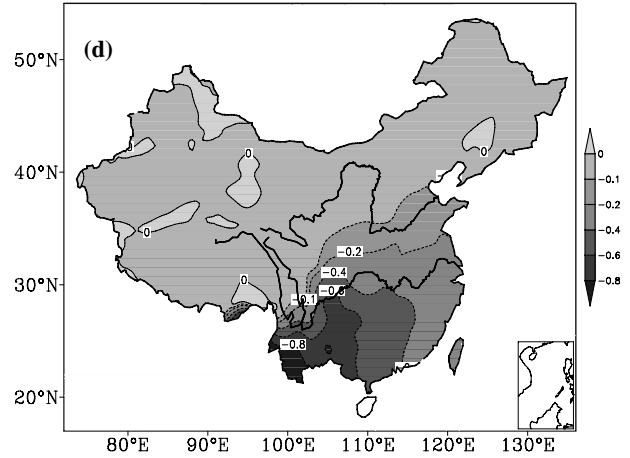
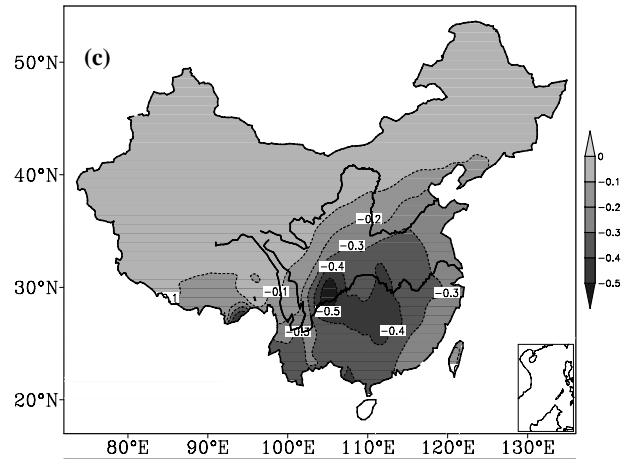
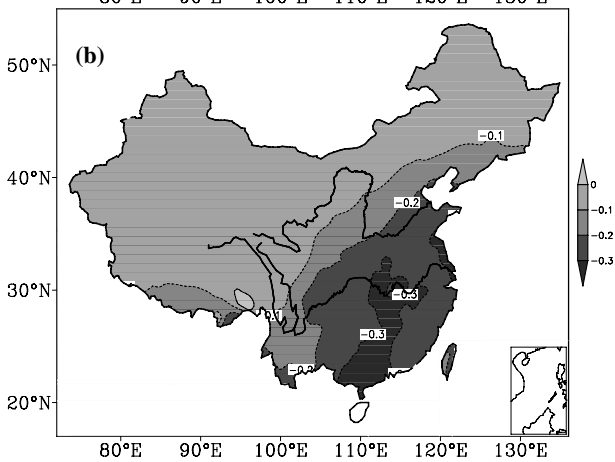
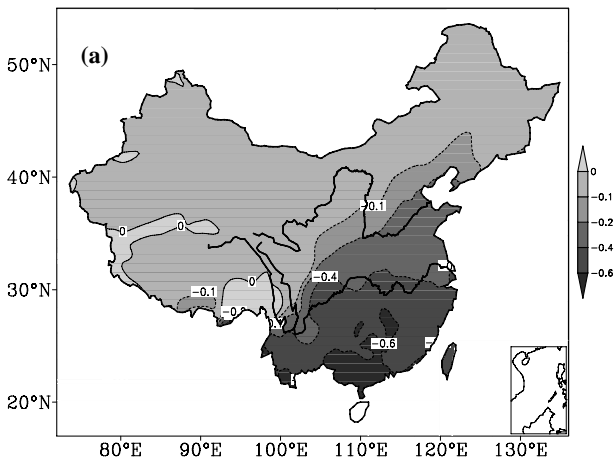


Figure 5. Seasonal averaged distribution of RF at the TOA (units: W/m^2). (a) spring; (b) summer; (c) autumn; (d) winter.

The RF of OC aerosols at the TOA in China is mostly between -0.1 and $-0.5 W/m^2$, and the mean value is about -0.30 to $-0.40 W/m^2$, which is comparable to the value reported by IPCC^[4]. The simulation results imply the accuracy of the parameterization of OC aerosols in RegCM3.

4.2 Radiative forcing at the surface

OC aerosols decrease solar radiation at the surface by scattering and absorbing sunlight, which leads to negative RF at the surface. The distribution characteristics of RF at the surface are similar to those at the TOA. Because of the similarity of distribution both at the surface and TOA, the yearly averaged distribution of RF at the surface is analyzed in order to reduce duplicity (Figure 6). The isoline of $-0.4 W/m^2$ is mainly located to the south of Yellow River and the east of Tibetan Plateau. The RF is more than $-0.6 W/m^2$ in most parts to the south of Yangtze River, and the maximum occurs in central southern China, south of China, Sichuan Basin, Yunnan province and southeast of Tibet with RF above $-1.0 W/m^2$. The distribution characteristics of RF at the surface are similar to that at the TOA, and the main divergence exists in the magnitude of RF at the surface, which is bigger than those at the TOA. Affected by southerly

summer monsoon, aerosols are driven into Jianghuai Basin, and the maximum of RF at the surface is expanded to northern China in summer, while it is concentrated in southern China in other seasons.

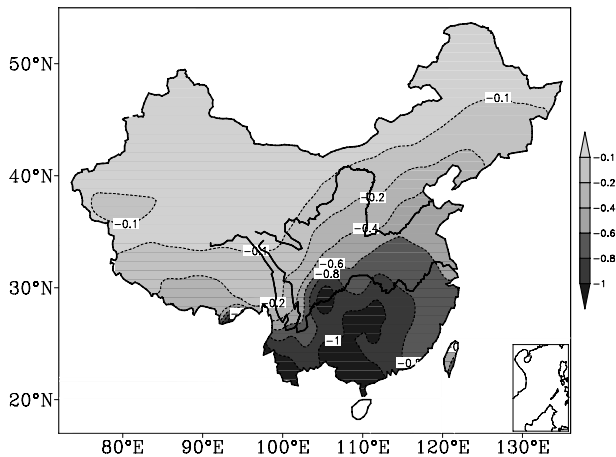


Figure 6. Yearly averaged distribution of RF at the surface (units: W/m^2).

Table 3. Regional averaged RF at the TOA and surface for different seasons (units: W/m^2).

Seasons	Spring	Summer	Autumn	Winter
RF at the TOA	-0.37	-0.20	-0.26	-0.36
RF at the surface	-0.84	-0.46	-0.55	-0.76

5 SUMMARY AND CONCLUSIONS

In this paper, the regional climate model RegCM3 is used to simulate spatio-temporal distribution characteristics and RF of OC aerosols in China. Preliminary simulation results are as follows.

(1) OC aerosols are mostly located to the south of Yellow River and east of Tibetan Plateau. There is a decreasing trend of column burden of OC aerosols from south to north. The maximum value of column burden of OC aerosols is above 3 mg/m^2 , which is located in southern China's Yunnan, Guizhou and Sichuan, central southern China and southeast of Tibetan Plateau. The column burden lower than 0.5 mg/m^2 is mainly located in northern Tibetan Plateau, northwestern China, most of northeastern China and Inner Mongolia Autonomous Region. The simulation on seasonal variation shows that the maximum value of column burden of OC aerosols appears in winter, and the secondary value is in spring and the minimum in summer. The existing of OC aerosols with high concentrations in southern Tibetan Plateau in China reflects the reality of transnational transportation of OC aerosols.

(2) The RF of OC aerosols is negative at the TOA. The maximum occurs in Guangxi, Yunnan and southeastern Tibet Autonomous Region with the value smaller than -0.5 W/m^2 , whereas the RF is between -0.1 and 0 W/m^2 in most of China including Tibetan

Plateau, Xinjiang and Mongolia Autonomous Region and northeastern China. The seasonal variation of RF of OC aerosols shows that the maximum value appears in southeastern China and southern China in spring and summer, and there is a descending trend from southeast to northwest. The spatio-temporal characteristics of the RF of OC aerosols are basically in consistency with its column burden. The simulated RF at the TOA is between -0.5 to -0.1 W/m^2 which is consistent with the IPCC's value of -0.41 W/m^2 .

(3) The RF of OC aerosols is negative at the surface, with the isoline of -0.4 W/m^2 located to the south of Yellow River and east of Tibetan Plateau. The RF smaller than -0.6 W/m^2 is identified in most of the region to the south of Yangtze River, and the maximum occurs in central southern China and south of China, Sichuan Basin, Yunnan and southeastern Tibet Autonomous Region.

(4) The seasonal variation of RF at TOA is the same as that at the surface. Although the maximum of column burden occurs in winter, the maximum of RF is found in spring. It indicates that the RF of OC aerosols is a very complex process and depends not only on the column burden but also other factors such as clouds, weather, atmospheric circulation, surface albedo, etc.

For the future work, improvements on parameterization of deposition, radiation and algorithm in calculating the RF of aerosols are still

needed to enhance the performance of the numerical models. Moreover, short lifetime (3 to 7days^[5] or 3.9 to 4.5 days^[6]) of OC aerosols, complex spatio-temporal distribution, lack of systematic observation of OC aerosols concentration constitute great uncertainties for simulated results.

REFERENCES:

- [1] MADER B T, SCHAUER J J, SEINFELD J H, et al. Sampling methods used for the collection of particle-phase organic and elemental carbon during ACE-Asia [J]. *Atmos. Environ.*, 2003, 37:1435-1449.
- [2] ZHOU Chang-wei, HUANG Hong, Cao Jun-ji. Review on basic characteristic of aerosols carbonaceous [J]. *Environ. Pollut. Control.*, 2006, 28(4): 270-274.
- [3] ZHANG Mei-gen, XU Yong-fu, PU Yi-fen, et al. Preliminary study on distribution characteristics of organic carbon aerosols over East Asia in the springtime [J]. *Chin. J. Process Eng.*, 2004, 4(Suppl.): 731-735.
- [4] IPCC. Third Assessment Report Climate Change 2001: the scientific basis [M]. Cambridge: Cambridge University Press, 2001.
- [5] HAN Z W, ZHANG R J, WANG Q G, et al. Regional modeling of organic aerosols over China in summertime [J]. *J. Geophys. Res.*, 2008, 113, D11202, doi: 10.1029/2007JD009436.
- [6] CAO G L, ZHANG X Y, ZHENG F C. Inventory of black carbon and organic carbon emissions from China [J]. *Atmos. Environ.*, 2006, 40: 6516-6527.
- [7] LÜ Zi-feng, HAO Ji-ming, LI Jun-hua, et al. Effect of calcium sulfate and ammonium sulfate aerosol on secondary organic aerosol formation [J]. *Acta Chimica Sinica*, 2008, 66(4): 419-423.
- [8] LIOUSSE C, PENNER J E, CHUANG C. A global three-dimensional model study of carbonaceous aerosols [J]. *J. Geophys. Res.*, 1996, 101: 19411-19432.
- [9] COOKE W F, LIOUSSE C, CACHIER H. Construction of a 1°×1° degree fossil fuel emission data set for carbonaceous aerosol and implementation and radiative impact in the ECHAM4 model [J]. *J. Geophys. Res.*, 1999, 104: 22137-22162.
- [10] STREETS D G, BOND T C, CARMICHAEL G R. An inventory of gaseous and primary aerosol emissions in Asia in the year 2000 [J]. *J. Geophys. Res.*, 2003, 108(21): 8809.
- [11] CHEN Gang-cai, YANG San-ming, ZHAO Qi, et al. Character of organic carbon and elemental carbon in Chongqing aerosols [J]. *Chongqing Environ. Sci.*, 2003, 25(10): 375-379.
- [12] YE Di, JIANG Chang-tan, ZHAO Qi, et al. Pollution character of organic carbon and elemental carbon in PM10 during springtime in Chongqing [J]. *Environ. Monit. China*, 2007, 23(3): 69-73.
- [13] XU Dian-dou, DAN Mo, SONG Yan, et al. Organic carbon and extractable organohalogens in Beijing atmospheric aerosols [J]. *China Environ. Sci.*, 2005, 25(Suppl.): 17-21.
- [14] MENG Zhao-yang, ZHANG Huai-de, JIANG Xiao-ming, et al. Characteristics of organic carbon and elemental carbon in PM2.5 during winter in Taiyuan [J]. *J. Appl. Meteorol. Sci.*, 2007, 18(4): 524-531.
- [15] CHENG Tian-tao, SHEN Zhi-bao. A numerical simulation of optical characteristics for atmospheric dust aerosols in Northwest China [J]. *Plateau Meteorol.*, 2001, 20(3): 291-297.
- [16] KIEHL J T, BRIEGLEB B P. The relative roles of sulfate aerosols and greenhouse gases in climate forcing [J]. *Science*, 1993, 260: 311-314.
- [17] International Center for Theoretical Physics. RegCM3 Data Web [DB/OL]. [2010-09-28] <http://users.ictp.it/~pubregcm/RegCM3/globedat.htm>.
- [18] ZHANG Jin, YIN Yan. Numerical simulations of effect of black carbon aerosol on regional climate in China [J]. *J. Nanjing Inst. Meteorol.*, 2008, 31(6): 852-859.
- [19] WU J, FU C B. Simulation Research of distribution transportation and radiative effects of black carbon aerosol in recent five spring seasons over East Asia region [J]. *Chin. J. Atmos. Sci.*, 2005, 29(1): 111-119.
- [20] JACOBSON M Z. Control of fossil-fuel particulate black carbon and organic matter, possibly the most effective method of slowing global warming [J]. *J. Geophys. Res.*, 2002, 107(19): 4410.
- [21] TAKEMURA T, OKAMOTO H, MARUYAMA Y. Global three-dimensional simulation of aerosol optical thickness distribution of various origins [J]. *J. Geophys. Res.* 2000, 105: 17853-17873.

Citation: SU Xing-tao, WANG Han-jie and ZHOU Lin. Simulation on spatio-temporal distribution characteristics and radiative forcing of organic carbon aerosols in China. *J. Trop. Meteorol.*, 2012, 18(3): 297-304.